Polymer 119 (2017) 134–141

Contents lists available at ScienceDirect

Polymer

journal homepage: www.elsevier.com/locate/polymer

# Polybenzimidazole based random copolymers containing hexafluoroisopropylidene functional groups for gas separations at elevated temperatures

Rajinder P. Singh [a, *], Xin Li [b], Kevin W. Dudeck [a], Brian C. Benicewicz [b], Kathryn A. Berchtold [a, **]

[a] Carbon Capture and Separations for Energy Applications (CaSEA) Labs, Materials Physics and Applications Division, Los Alamos National Laboratory, Los Alamos, NM 87545, United States
[b] Department of Chemistry and Biochemistry, University of South Carolina, Columbia, SC 29208, United States

ARTICLE INFO

*Article history:*
Received 23 February 2017
Received in revised form
23 April 2017
Accepted 27 April 2017
Available online 28 April 2017

*Keywords:*
Polybenzimidazole
Random copolymer
Pre-combustion
Carbon capture
Synthesis gas
Hydrogen selective membrane

ABSTRACT

Polybenzimidazoles (PBIs) are attractive membrane materials for $H_2/CO_2$ separation at hydrocarbon fuel derived synthesis gas operating conditions due to their exceptional physicochemical stability and promising permselectivity character. PBI molecular structure modification is a viable approach to disrupt chain packing altering the free-volume architecture which results in improved gas transport characteristics. This work is focused on the synthesis and characterization of novel PBI random copolymers for application as elevated temperature $H_2/CO_2$ membranes. The co-polymerization route is expected to result in tailorable permeability and selectivity by combining the high $H_2$ permeability aspect of the highly disrupted loosely packed hexafluoroisopropylidene diphenyl group containing PBI segments (6F-PBI) with the highly selective tightly packed phenylene group containing PBI segments (m-PBI). 6F/m-PBI copolymers with varying 6F-PBI and m-PBI ratios having high inherent viscosity were synthesized. The structure and ratio of the 6F- and m-PBI fractions were confirmed using FTIR and NMR spectroscopic techniques. The measured gas transport properties of copolymer thin films cast in controlled environment were measured as a function of the operating conditions. The $H_2$ permeability increased while $H_2/CO_2$ selectivity decreased as the 6F-PBI copolymer fraction was increased.

© 2017 Elsevier Ltd. All rights reserved.

## 1. Introduction

High temperature $H_2$-selective membranes are ideally suited for pre-combustion $H_2/CO_2$ separations in an advanced hydrocarbon fuel processing schemes for power, fuels and chemicals production. Synthesis gas, predominantly a mixture of $H_2$, $CO_2$ and steam with trace impurities, produced in hydrocarbon fuel processing scheme in the vicinity of water gas shift reactors is typically at elevated temperatures (ca. 250–350 °C). Since the efficiency of the advanced hydrocarbon fuel processing scheme with integrated carbon capture is strongly tied to efficient process integration, $H_2$ selective membranes for $H_2/CO_2$ separations with tolerance to syngas operating conditions and chemical environments are required [1–3].

Commercially available polymeric membranes typically lack the thermal and chemical tolerances required for energy efficient syngas separations at elevated temperatures exceeding 150 °C. Polybenzimidazole (PBI)-based materials are a class of heterocyclic polymers with exceptional thermal stability, chemical tolerance and solution processability. These characteristics make PBI an attractive membrane material for use in gas, vapor and liquid separation applications in challenging industrial operating environments including high temperatures and in the presence of steam, sulfur compounds, CO and other impurities.

Owing to the microstructural rigidity imparted by efficient π-π stacking and strong H-bonding, PBI demonstrates promising molecular sieving characteristics for efficient $H_2/CO_2$ separation at elevated temperatures [4,5]. The high $H_2/CO_2$ perm-selectivity of commercially available PBI materials has been demonstrated by testing a PBI-metallic composite membrane for gas permeation at

* Corresponding author.
** Corresponding author.
*E-mail addresses:* rsingh@lanl.gov (R.P. Singh), berchtold@lanl.gov (K.A. Berchtold).

http://dx.doi.org/10.1016/j.polymer.2017.04.075
0032-3861/© 2017 Elsevier Ltd. All rights reserved.

250 °C for approximately 1 year [4]. In addition, the solution processability of PBI allows fabrication of industrially deployable PBI hollow fiber membranes providing high surface area to volume modules for large scale $H_2/CO_2$ separations [6,7].

The $H_2$ permeability characteristics of commercially available PBI materials mandate a thin defect-free selective layer to achieve high throughputs which is an industrial challenge. Therefore, designing novel PBI-based materials via molecular structure manipulation or material combinatorial engineering approaches to improve the $H_2$ perm-selectivity character is an attractive research topic. Chemical modification of polymer structure at a molecular level is a widely studied approach towards improving the intrinsic gas separation properties of polymeric materials. For example, this approach has been used to great effect for polyimide gas transport property manipulation [8,9]. However, only a few studies have explored PBI molecular structural variation strategies to achieve better gas separation performances [10–12]. Other material engineering routes; 1) blending with other thermally robust polymers such as melamine-co-formaldehyde [13] and polyimide [14], 2) post-synthesis N-H group modification [15–17], 3) thermal rearrangement [18], and 4) incorporation of high permeable fillers such as zeolitic imidazole frameworks (ZIFs) [19,20] were also explored to manipulate the $H_2$ perm-selectivity character of PBI materials.

Our efforts are focused on the influence of PBI main chain molecular modifications for elevated temperature gas transport characteristics. We previously reported the elevated temperature gas permeation properties of four PBI derivatives with main chain molecular structure variations as compared to m-PBI. These PBI materials incorporated high localized mobility at elevated temperatures, rigid and bent configurations that frustrated close chain packing, and/or bulky side groups. These main chain structural variations effectively disrupted the PBI chain packing resulting in significantly improved $H_2$ permeability (up to 997.2 barrer) compared with m-PBI (76.81 barrer) at 250 °C and 50 psia. However, lower $H_2/CO_2$ selectivities (5–7 (modified PBIs) versus 23 (m-PBI)) were also measured. This inverse trend in $H_2$ permeability and $H_2/CO_2$ selectivity reflected the general trade-off between gas permeability and selectivity typically observed for polymer membranes [21].

In that same study, PBI derivatives containing the hexafluoroisopropylidene diphenyl group (6F-PBI) exhibited approximately one order of magnitude higher $H_2$ permeability at 250 °C but lower $H_2/CO_2$ selectivity as compared to the phenylene group containing m-PBI [10]. It is hypothesized here that the $H_2$ perm-selectivity of PBI materials can be further controlled by manipulating the 6F-PBI content of those materials. In order to optimize the complementary properties of gas permeability and selectivity, initial efforts employed a solution blending approach to prepare new PBI derivatives. However, only poor quality PBI membranes were obtained using this simple mixing approach due to phase separation during the solvent evaporation process. Therefore, the focus of this work was to utilize copolymerization to tailor PBI membrane performance; leveraging the gas transport characteristics of the highly permeable hexafluoroisopropylidene diphenyl containing 6F-PBI with those of the highly selective m-phenylene containing m-PBI. PBI-based random copolymers containing hexafluoroisopropylidene diphenyl and m-phenylene groups in varying molar ratios were successfully synthesized. The optimum conditions for co-polymer synthesis and spectroscopic chemical structure characterization to ascertain macromolecular structure and the co-polymer component fractions are reported. The pure gas permeation characteristics of co-polymer thin films were evaluated at elevated temperatures as a function of the pressure gradient across the membrane.

## 2. Experimental

### 2.1. Materials

2,2-Bis(4-carboxyphenyl)-hexafluoropropane (6F-diacid, 98.0%) was purchased from TCI America. Isophthalic acid (IPA, purified) was purchased from Amoco Chemicals. 3,3′,4,4′-Tetraaminobiphenyl (TAB, polymer grade, ~97.5%) was donated by BASF Fuel Cell, Inc. Polyphosphoric acid (PPA, 115%) was purchased from InnoPhos, Inc. All other reagents (e.g. lithium chloride (99%)) and solvents (e.g., *N*,*N*-dimethylacetamide (DMAc), 1-methyl-2-pyrrolidinone (NMP), ammonium hydroxide) were purchased from Fisher Scientific, Inc. For comparison, m-PBI material obtained from PBI Performance Products, Inc in solution form (26.2 wt% PBI in dimethylacetamide containing 2 wt% lithium chloride) was used as the benchmark PBI material for gas transport measurements. Unless otherwise specified, all chemicals were used without further purification.

### 2.2. Synthesis of 6F/m-PBI random copolymers

The synthesis procedure for neat 6F-PBI polymer is reported in our previous publication [10]. The general procedure for the synthesis of 6F/m-PBI random copolymers (e.g. 6F/m = 50/50, mol/mol) is described as follows: A 100 ml, three-necked, round-bottom flask equipped with an overhead mechanical stirrer, and $N_2$-purge inlet and outlet was used. TAB (2.681 g, 12.50 mmol), IPA (1.039 g, 6.25 mmol), and 6F-diacid (2.454 g, 6.25 mmol) were charged to the reactor in a $N_2$ glove box, followed by 124 g of PPA (Fig. 1). The mixture was then stirred by the mechanical stirrer set at 50 rpm and purged under flowing $N_2$. The reaction temperature (oil bath temperature) was controlled by a programmable temperature controller. A multi-stage temperature profile with intermediate temperatures of 140–185 °C and final polymerization temperatures of 195–220 °C was utilized to synthesize each batch of copolymer. The heating profiles for each co-polymer synthesis are given in Table 1. The temperature profiling was used to minimize the sublimation of the di-acid monomer. As the reaction proceeded, the solution became more viscous and developed a dark brown color. At the end of the polymerization, the polymer solution was poured into DI water, pulverized, neutralized with ammonium hydroxide, and vacuum dried at 110 °C overnight to obtain the polymer powders.

### 2.3. PBI dense membrane preparation

The optimized procedure for the PBI-based dense membrane preparation as described by Xin et al. [10] is briefly described here. For each copolymer formulation, approximately 1 g of PBI powder was mixed with 30 ml of *N*,*N*-dimethylacetamide (DMAc) in a 100 ml round bottom flask and then refluxed for 2–3 h until most of the polymer was dissolved. After refluxing, the undissolved polymer, if any, was removed by centrifugation at 6000 rpm for 0.5 h to obtain clear PBI solution. The PBI solutions were transferred to a glove bag and three evacuation/$N_2$ purge cycles were applied before casting. The dense PBI films were cast onto a clean glass substrate under dry $N_2$ atmosphere to avoid polymer precipitation due to ambient moisture absorption. After casting, the wet films were pre-dried under $N_2$ atmosphere on a hot-plate at approximately 40 °C (hot plate temperature) overnight to remove solvent. Then the films were dried in a vacuum oven at 120 °C overnight. Finally, the PBI films were peeled from the glass substrate.

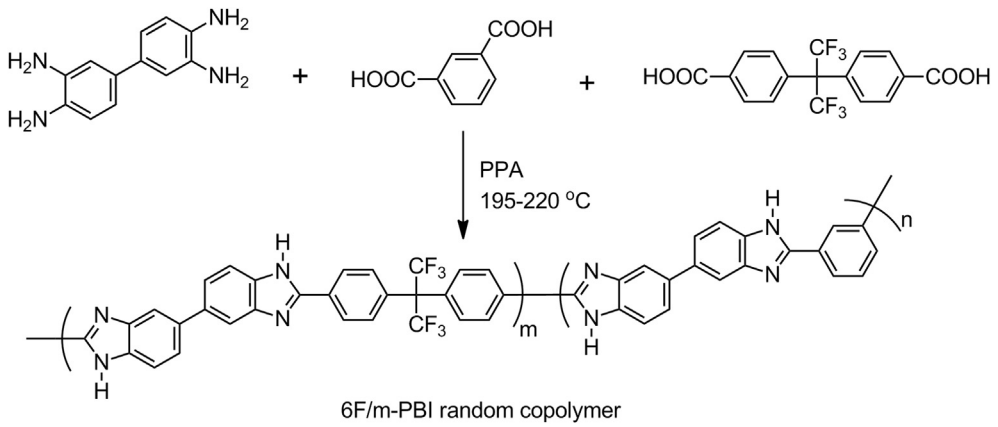


**Fig. 1.** Synthesis of 6F/m-PBI random copolymers.

**Table 1**
Synthetic details of 6F/m-PBI random copolymer.

| Polymer | Monomer loading (wt%) | Time at polymerization temperature (h) | | | | | IV (dL/g) |
|---|---|---|---|---|---|---|---|
| | | 140 °C | 170 °C | 185 °C | 195 °C | 220 °C | |
| 6F/m-PBI (50:50) | 4.74 | 2 | 4 | 16 | 17 | 15 | 1.96 |
| 6F/m-PBI (25:75) | 5.62 | 13 | 22 | 16 | 17 | 20 | 2.22 |
| 6F/m-PBI (10:90) | 6.10 | 14 | 15 | 15 | 14 | 10 | 1.26 |

### 2.4. Characterization

$^1$H NMR spectra were recorded on a Varian Mercury 400 spectrometer. Deuterated DMSO (DMSO-$d_6$) was used as solvent for NMR characterization. FTIR spectra were recorded on a PerkinElmer Spectrum 100 FT-IR spectrometer in ATR mode. The inherent viscosities (IVs) of the polymer samples were measured using a Cannon Ubbelohde viscometer at a polymer concentration of 0.2 g/dL in concentrated sulfuric acid (96 wt%) at 30 °C (water bath temperature). The PBI solubilities were evaluated at ambient and at refluxing conditions. At ambient temperature, the PBIs were mixed with each solvent and shaken on a wrist action shaker for at least 48 h. At high temperature, the PBIs were mixed with each solvent and then refluxed for 4–6 h. Thermogravimetric analysis (TGA) was conducted on polymer powders using a TG209F1 Iris from Netzsch Inc. The samples were heated at 200 °C for 12 h to ensure residual solvent and sorbed water removal prior to thermal analysis. After the drying step, samples were heated at a ramp rate of 2 °C/min in $N_2$ from 75 to 1000 °C. The gas permeation characteristics of the PBI membranes were measured in a constant-volume variable-pressure test system discussed in detail in our previous publication [10]. Both gas permeability and ideal selectivity were measured as a function of temperature (30–250 °C) and feed pressure (20–50 psi).

## 3. Results and discussion

### 3.1. Polymer synthesis

PPA has been widely used in PBI synthesis since it serves as both solvent and dehydrating agent, and produces high molecular weight polymers [22,23]. Therefore, PPA was chosen here for high molecular weight homopolymer and random copolymer syntheses. The details of the polymerization conditions are given in Table 1. The synthetic details of 6F-PBI homopolymerization in PPA were studied and reported previously [24,25]. A modified multi-step temperature control profile with additional intermediate reaction temperatures was found to be key to both suppress 6F-diacid monomer sublimation and produce high molecular weight polymer. A similar temperature profile was also applied herein and high molecular weight 6F-PBI homopolymer (IV = 1.40 dL/g) was produced. Due to the poor solubility of PBI polymers in most common organic solvents, it is difficult to characterize their molecular weight using regular techniques, such as GPC/SEC. The molecular weight of PBI is usually analyzed via inherent viscosity (IV) measurement by dissolving the polymer in strong inorganic acid (i.e. sulfuric acid). Yuan et al. reported linear correlation between IV and molecular weight determined by light scattering measurement for PBI with slight deviation (within 3%) from linearity at IVs exceeding 1.2 [26]. Although, polymer interactions with sulfuric acid can influence the IV measurement, this method is well-accepted by the scientific community for the purpose of making relative comparisons. Shogbon et al. conducted molecular weight characterization of m-PBI (IV = 1.59 dL/g) using static light scattering technique by dissolving the polymer in DMAc/LiCl solvent and obtained a weight-average molecular weight ($M_w$) of 199,200 Da, indicating high molecular weight in this class of polymers having IVs $\geq$ 1 [27]. A series of 6F/m-PBI random copolymers (6F/m = 50/50 to 10/90 mol/mol) were synthesized by adjusting the feed ratio of the two diacid monomers. Previous studies indicated that IPA has much higher solubility in PPA than 6F-diacid and the optimal monomer loading for a typical m-PBI homopolymerization in PPA (~8.3 wt%) is much higher than that for 6F-PBI (~3.0 wt%) [25,28]. In this work, the monomer loading for the random copolymerization was gradually increased (from 4.74 to 6.10 wt%) with the increase in the ratio of m-PBI in the final random copolymers. This process was followed to achieve high monomer reactivity and polymer molecular weight. All the random copolymers produced exhibited relatively high IVs ranging from 1.3 to 2.2 dL/g, indicating high polymer molecular weight.

### 3.2. Polymer characterization

The FTIR spectra of PBI derivatives exhibit common absorptions

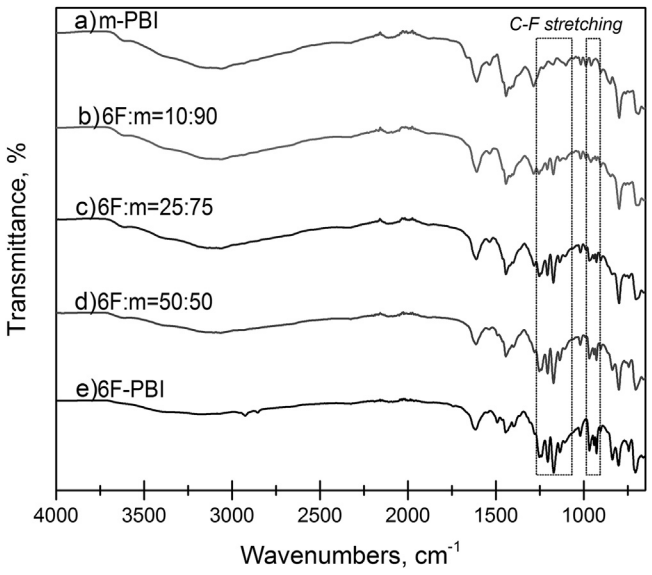


**Fig. 2.** FTIR spectra of PBI derivatives (a: m-PBI; b: 6F/m-PBI copolymers (10/90); c: 6F/m-PBI copolymers (25/75); d: 6F/m-PBI copolymer (50/50); e: 6F-PBI).

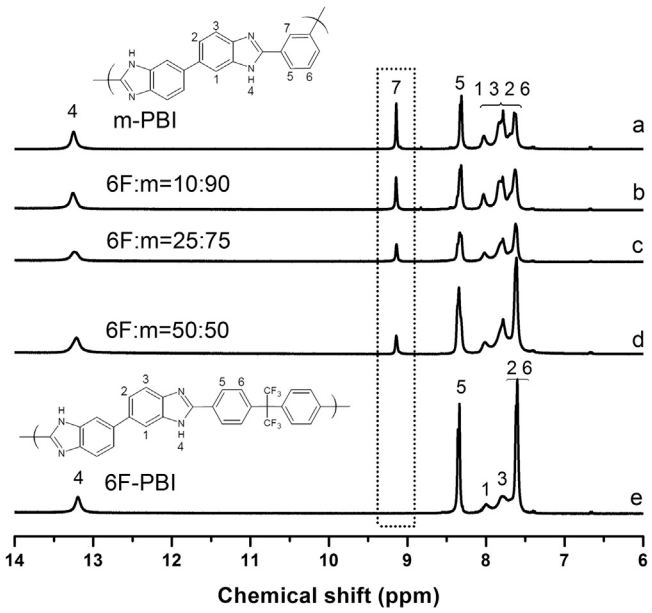


**Fig. 3.** $^1$H NMR spectra of PBI derivatives (a: m-PBI; b: 6F/m-PBI copolymers (10/90); c: 6F/m-PBI copolymers (25/75); d: 6F/m-PBI copolymer (50/50); e: 6F-PBI).

at 3500-2800 cm$^{-1}$, 1600 cm$^{-1}$, 1430 cm$^{-1}$, and 1410 cm$^{-1}$ (Fig. 2). The broad band at ~3150 cm$^{-1}$ corresponds to the stretching vibration of hydrogen bonded N-H•••H groups [29]. The region 1650-1400 cm$^{-1}$ is characteristic of the benzimidazole ring and these bands are attributed to the C=C and C=N stretching, in-plane ring vibration of benzimidazole and imidazole ring breathing modes. In the spectrum of the 6F-PBI homopolymer, broad absorption peaks at 927-969 cm$^{-1}$ and 1104-1268 cm$^{-1}$ are observed and attributed to C-F stretching vibrations. In the case of 6F/m-PBI random copolymers, increasing signal strength at these C-F stretching vibration bands is clearly observed with the increasing component ratio of 6F-PBI in 6F/m-PBI random copolymers. Additionally, the systematic decrease in the broad band at ca. 3150 cm$^{-1}$ is attributable to changes in the extent of H-bonding in the co-polymer system due to introduction of increasing amounts of bulky, hydrophobic 6F moieties. This indirect evidence suggests that the polymer packing efficiency, directly affected by H-bonding, can be controlled by adjusting the m and 6F monomer ratios.

The synthesized 6F/m-PBIs were also characterized by $^1$H NMR and the results are shown in Fig. 3. Common proton peaks representing the benzimidazole unit are observed including imidazole protons ($H_4$; 12.7–13.5 ppm) and biphenyl protons ($H_1$, $H_2$, and $H_3$; 7.5–8.2 ppm). The decreasing signal strength of the m-PBI characteristic peak ($H_7$; 9.13 ppm) is clearly observed with the increasing component ratio of 6F-PBI in the copolymers. A precise quantitative co-polymer composition was not determined due the common peaks of the m- and 6F- moieties and poor peak resolution. Typically, the final co-polymer composition in step-growth polymerization is very close to initial monomer feed. High purity monomer (kindly supplied by the manufacturer) was used in these syntheses resulting in high IV co-polymers. These high IV polymerization results indicate that stoichiometry was maintained during polymerization as the presence of impurities and correspondingly loss of adherence to the reactant stoichiometry typically leads to a significant drop in polymer IV. Both FT-IR and NMR characterization confirmed the successful synthesis of 6F/m-PBI copolymers with varied component ratios.

The solubility characteristics of these PBIs were determined in two different conditions: a) 1.5 and 5.0 wt% polymer concentrations at ambient temperature; b) 5.0 wt% polymer concentration at reflux temperature. The results of these solubility tests are given in Table 2. All PBIs evaluated were soluble in concentrated sulfuric acid at ambient temperature. These polymers also dissolved or partially dissolved in certain polar aprotic solvents such as DMAc, DMAc/LiCl, and NMP. 6F-PBI was reported to exhibit much better solubility than m-PBI in these solvents, which is attributed to the introduction of bulky, flexible fluorinated functional groups into the polymer main chain. As the molar ratio of 6F-PBI in the random copolymers increased from 10% to 50%, the solubility slightly increased. All the PBIs are insoluble in common organic solvents

**Table 2**
Solubility characteristics of PBI derivatives.

| Polymer | Inherent viscosity | Feed ratio (6F:m) | Ambient temperature | | | | | | | | | Reflux temperature | |
|---|---|---|---|---|---|---|---|---|---|---|---|---|---|
| | | | $H_2SO_4$ | DMAc/LiCl | | DMAc | | NMP | | THF | MeOH | DMAc/LiCl | DMAc |
| | | | 1.5 wt% | 1.5 wt% | 5 wt% | 1.5 wt% | 5 wt% | 1.5 wt% | 5 wt% | 1.5 wt% | 1.5 wt% | 5 wt% | 5 wt% |
| 6F/m-PBI | 1.26 | 10:90 | ++ | ++ | ++ | ++ | + | ++ | + | - | - | ++ | + |
| 6F/m-PBI | 2.22 | 25:75 | ++ | ++ | ++ | ++ | + | ++ | + | - | - | ++ | ++ |
| 6F/m-PBI | 1.96 | 50:50 | ++ | ++ | ++ | ++ | + | ++ | + | - | - | ++ | ++ |
| 6F-PBI | 1.40 | N/A | ++ | ++ | ++ | ++ | ++ | ++ | ++ | - | - | ++ | ++ |

1) DMAc: *N*, *N*-dimethylacetamide; DMAc/LiCl: 4 wt% LiCl in DMAc; NMP: *N*-methyl-2-pyrrolidinone; THF: tetrahydrofuran; MeOH: methanol.
2) ++: mostly soluble; +: partially soluble or swelling; -: insoluble (by visual observation).

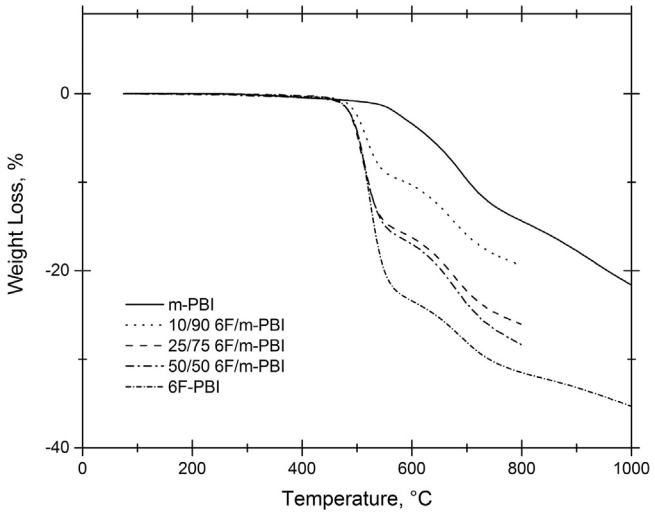


**Fig. 4.** TGA thermograms of m-PBI, 6F-PBI, and 6F/m-PBI random copolymers.

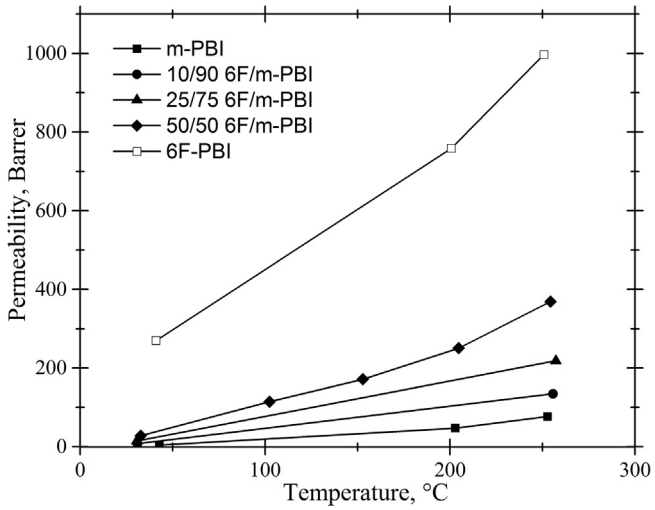


**Fig. 5.** $H_2$ permeability as a function of operating temperature for m-PBI, 6F-PBI and 6F/m-PBI copolymers. Data obtained at $P_{feed}$ = 50 psia. Lines are shown to guide the eye.

**Table 3**
Gas permeation properties of 6F-PBI, m-PBI and 6F/m-PBI copolymers measured at 250 °C and 50 psia. For comparison, data for neat 6F-PBI and m-PBI polymers is taken from Xin et al. [10].

| Polymer | $H_2$ Permeability, barrer | Selectivity | | |
|---|---|---|---|---|
| | | $H_2/CO_2$ | $H_2/N_2$ | $CO_2/N_2$ |
| 0/100: 6F/m-PBI | 76.8 | 23.0 | 98.3 | 4.27 |
| 10/90: 6F/m-PBI | 136 | 13.6 | 52.7 | 3.88 |
| 25/75: 6F/m-PBI | 219 | 11.1 | 45.8 | 4.13 |
| 50/50: 6F/m-PBI | 371 | 8.21 | 32.2 | 3.92 |
| 100/0: 6F/m-PBI | 997 | 5.17 | 18.7 | 3.62 |

such as THF and MeOH.

The thermal stability of 6F/m-PBI copolymers was studied using TGA under $N_2$. Polymer powders were pre-treated *in-situ* at 200 °C for 12 h in the TGA to remove residual solvent and sorbed water. As shown in Fig. 4, 6F/m-PBI copolymers exhibit excellent thermal stability with no obvious weight loss (<1 wt%) observed at temperatures up to 400 °C. The thermal stability of m-PBI is greater than 6F-PBI and as the fraction of 6F-PBI in the copolymer increased the weight loss profile changed as anticipated by the increased presence of 6F-PBI segments. Correspondingly, the weight loss profile of 6F/m-PBI copolymers falls within the upper and lower bounds created by m-PBI and 6F-PBI. The demonstrated thermal stability of 6F/m-PBI co-polymers to 400 °C indicates their suitability for elevated temperature $H_2/CO_2$ separations at syngas operating temperatures (ca. 250–350 °C) in the vicinity of WGS reactors. The glass transition temperature (Tg) was not detectible in this class of polymers in differential scanning calorimetry (DSC) up to 400 °C [25]. At temperatures above 400 °C, the onset of thermo-degradation of each co-polymer was observed.

### 3.3. Gas permeation

Pure gas permeation data were measured at varying feed pressures and operating temperatures for the 6F/m-PBI copolymer films and compared to the previously reported gas permeation properties of the neat m-PBI and 6F-PBI films. Table 3 reports the gas permeation properties of 6F-PBI and m-PBI homopolymers, and 6F/m-PBI copolymers measured at 250 °C and 50 psia. The highest $H_2$ permeability and lowest $H_2/CO_2$ and $H_2/N_2$ selectivities were measured for 6F-PBI whereas the lowest $H_2$ permeability and highest $H_2/CO_2$ and $H_2/N_2$ selectivities were measured for m-PBI. As the molar ratio of 6F-PBI in the 6F/m-PBI co-polymer is increased from 10 to 50, the $H_2$ permeability increases while $H_2/CO_2$ and $H_2/N_2$ selectivities decrease.

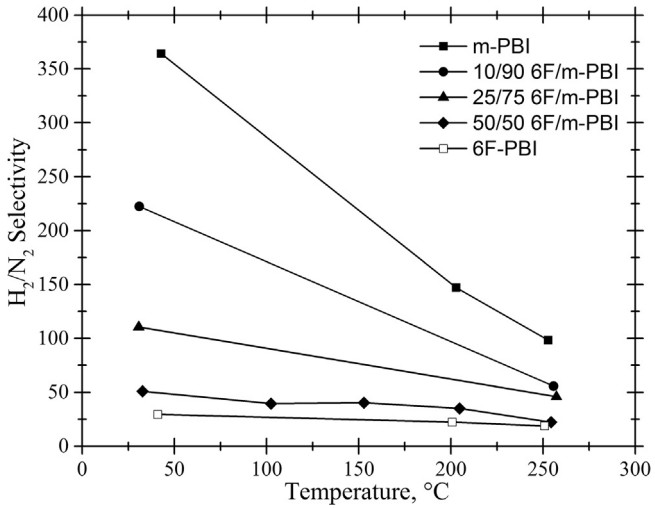


**Fig. 6.** $H_2/N_2$ selectivity as a function of operating temperature for m-PBI, 6F-PBI and 6F/m-PBI copolymers. Data obtained at $P_{feed}$ = 50 psia. Lines are shown to guide the eye.

As mentioned above, PBI forms a tightly packed polymer network due to its rigid macromolecular structure with extensive π-π stacking and H-bonding sites. This efficient packing results in the efficient $H_2/CO_2$ separation characteristics of PBI. The presence of two types of free-volume cavities can be envisioned for the co-polymers – large and small cavities created by packing of 6F-PBI and m-PBI segments, respectively. As the 6F-PBI segment fraction is increased, the fraction of larger cavities is also increased resulting in the enhanced permeability and reduced $H_2/CO_2$ selectivity.

Figs. 5–7 show the $H_2$ permeability and $H_2/N_2$ and $H_2/CO_2$ selectivities, respectively, as a function of operating temperature for m-PBI, 6F-PBI and 6F/m-PBI copolymers. The $H_2$ permeability increased as operating temperature increased from near ambient to 250 °C for all membranes. The increase in $H_2$ permeability with

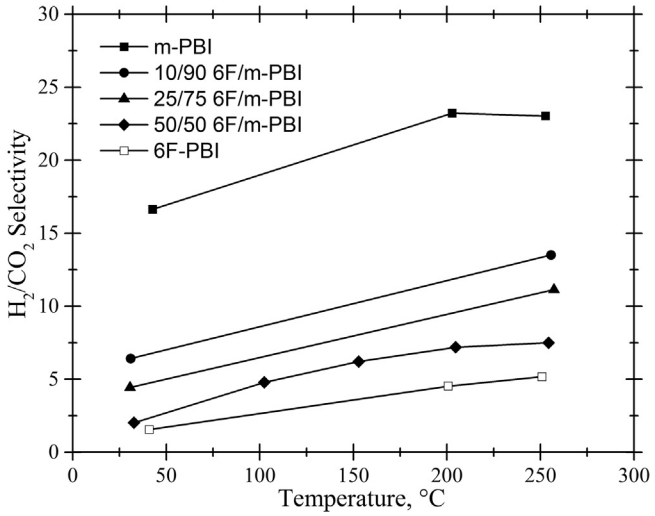


**Fig. 7.** $H_2/CO_2$ selectivity as a function of operating temperature for m-PBI, 6F-PBI and 6F/m-PBI copolymers. Data obtained at $P_{feed}$ = 50 psia. Lines are shown to guide the eye.

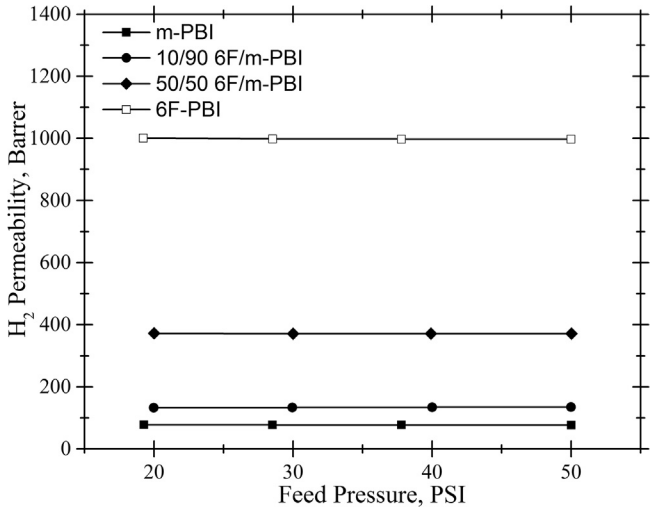


**Fig. 8.** $H_2$ permeability as a function of feed pressure for m-PBI, 6F-PBI and 6F/m-PBI copolymers obtained at 250 °C.

increasing temperature is dependent on the polymer and correlated well with the fraction of 6F-PBI. Quantitatively, the impact of temperature on $H_2$ permeability is observed in the activation energy for permeability as calculated using Equation (1).

$$P = P_0 e^{-E_p/RT} \quad (1)$$

where $E_p$ (KJ/mol) is the activation energy for permeability, R (8.314 J/mol) is the universal gas constant, and T (K) is temperature. The activation energies calculated from $H_2$ permeability versus temperature for each material composition are: m-PBI = −19.35, 10/90 6F/m-PBI = −17.07, 25/75 6F/m-PBI = −16.02, 50/50 6F/m-PBI = −15.23, and 6F-PBI = −8.36 KJ $mol^{-1}$. The observed decrease in activation energies as the 6F-PBI fraction is increased indicates that lower energy is required for $H_2$ transport through 6F-PBI than m-PBI. This activation energy trend is attributed to chain packing disruption and large cavity creation by the hexafluoro isopropylidenediphenyl groups on 6F-PBI segments.

Interestingly, $H_2/N_2$ selectivity decreases with temperature

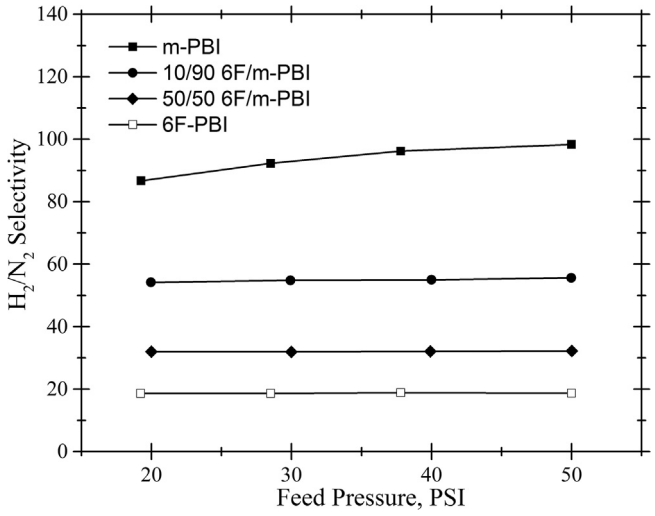


**Fig. 9.** $H_2/N_2$ selectivity as a function of feed pressure for m-PBI, 6F-PBI and 6F/m-PBI copolymers obtained at 250 °C.

whereas $H_2/CO_2$ selectivity increases with temperature for all polymers evaluated in this study. The observed decrease in $H_2/N_2$ selectivity is consistent with activated diffusion in glassy polymers. The selectivity of glassy polymers often decreases with temperature as a less permeable gas component often possesses higher activation energies, i.e., these less permeable gases realize relatively larger increases in permeability with increasing temperature. The temperature dependence of the ideal $H_2/N_2$ selectivity for these PBI membranes follows this general trend. Besides activated diffusion, the polymer chain motion (rotational and vibrational) is significantly influenced at elevated temperatures. Since polymer free volume is a function of polymer chain packing and intersegmental motion, the increased $N_2$ permeability is also influenced by the effect of elevated temperature on these aforementioned polymer macromolecular characteristics. In contrast, the $H_2/CO_2$ ideal selectivities increase with temperature resulting from a larger increase in $H_2$ permeability as a function of temperature compared to that of $CO_2$. The relatively large increase in $H_2$ permeability compared to $CO_2$ with temperature is attributed to its smaller size consistent with the size sieving characteristics of PBI. In addition, the solubility driven permeability component, the minor component in these PBI materials, is expected to be higher for $CO_2$ as compared to $H_2$ due to higher $CO_2$ solubility in the polymer. However, this solubility component decreases with increasing temperature thereby further contributing to an increase in $H_2/CO_2$ selectivity.

Figs. 8–10 show the effect of feed pressure on $H_2$ permeability and $H_2/N_2$ and $H_2/CO_2$ selectivity of the m-PBI, 6F-PBI and 6F/m-PBI copolymers at 250 °C. The gas permeability is identical as a function of pressure for all membranes tested. Since solubility is anticipated to have minimal effect on gas permeance at these elevated temperatures, a constant permeability indicates the absence of pressure dependent viscous flow which is typically caused by film or membrane module defects.

The selectivity and permeability trade-off curve is a common method to compare performance of polymer membranes. Fig. 11 shows the trade-off curve for PBI-based polymer materials tested in this and previous work both for permeation data measured at near ambient (30–40 °C) and elevated (250 °C) temperatures. In general for all the evaluated PBI membrane materials, the $H_2/CO_2$ selectivity decreased as $H_2$ permeability increased both at near ambient and elevated temperatures. This observed perm-

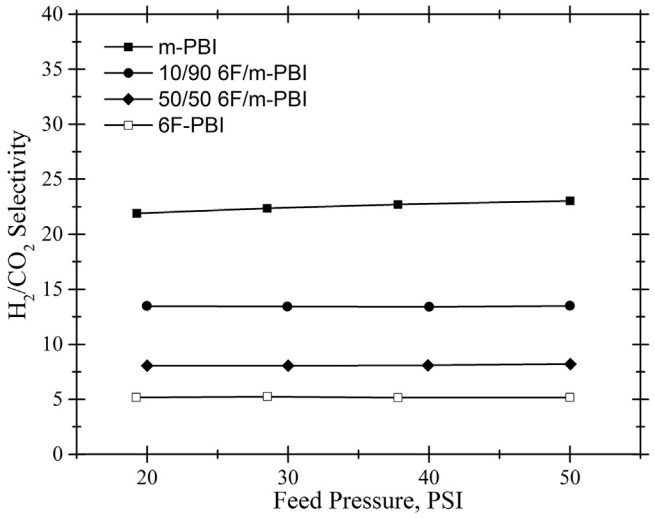


**Fig. 10.** $H_2/CO_2$ selectivity as a function of feed pressure for m-PBI, 6F-PBI and 6F/m-PBI copolymers obtained at 250 °C.

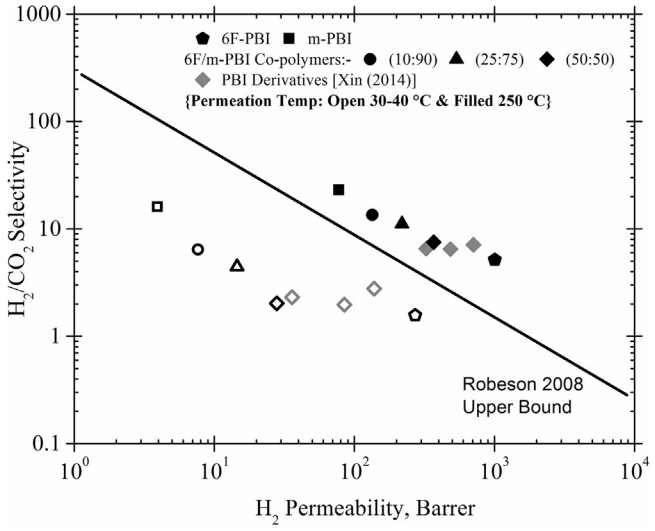


**Fig. 11.** $H_2/CO_2$ separation performance of 6F/m-PBI random copolymers in comparison to other polymeric materials. Ref: Xin et al. [10] and Robeson [21].

selectivity trend for PBI materials is consistent with trends typically observed for polymer membranes presented by the "Robeson 2008 Upper bound" line in Fig. 11 [21]. The perm-selectivity of 6F/m-PBI copolymers falls within the upper and lower bound created by m-PBI and 6F-PBI homopolymers, respectively, indicating that copolymerization is a viable route to tailor the perm-selectivity character of PBI materials.

## 4. Conclusions

Random PBI copolymer membranes containing hexafluoroisopropylidene diphenyl and m-phenylene groups were synthesized and evaluated for their gas separation performance as a function of the operating conditions. A polyphosphoric acid (PPA) solution polymerization process was used to control the ratio of 6F and m-PBI fractions in the copolymers while achieving the high molecular weight (high IV) polymers necessary for defect-free mechanically strong film formation. FT-IR and NMR studies conducted on the synthesized polymers provided evidence of successful variation in the ratios of m-PBI and 6F-PBI fractions. The $H_2$ permeability of 6F/m-PBI copolymer films increased as the fraction of 6F-PBI was increased from 10 to 50 mol%. Conversely, the $H_2/CO_2$ and $H_2/N_2$ selectivity decreased as the 6F-PBI fraction was increased. The $H_2/CO_2$ separation performance of these copolymers surpassed the 2008 Robeson upper bound at 250 °C demonstrating an excellent fit for elevated temperature hydrogen/syngas separations in comparison to other polymeric membranes tested for this application. Additionally, the copolymer approach allows for tailoring the selectivity/permeability balance in the design of membranes for various separation processes.

## Acknowledgements

This project supports the U.S. DOE Energy Efficiency and Renewable Energy – Advanced Manufacturing Office – Industrial Technologies Program. The authors gratefully acknowledge the U.S. DOE/EERE-AMO-ITP for financial support of the project under contract CPS #18990. Los Alamos National Laboratory is operated by Los Alamos National Security, LLC for DOE/NNSA under Contract DE-AC52-06NA25396. The authors also acknowledge PBI Performance Products Inc. for their programmatic contributions.

## References

[1] J.J. Marano, J.P. Ciferino, Integration of gas separation membranes with IGCC identifying the right membrane for the right job, Energy Proc. 1 (2009) 361–368.
[2] J.M. Klara, J.E. Plunkett, The potential of advanced technologies to reduce carbon capture costs in future IGCC power plants, Int. J. Greenh. Gas Con. 4 (2010) 112–118.
[3] R.P. Singh, K.A. Berchtold, $H_2$ selective membranes for precombustion carbon capture, in: F. Shi, B. Morreale (Eds.), Novel Materials for Carbon Dioxide Mitigation Technology, Elsevier, Amsterdam, 2015, pp. 177–206.
[4] K.A. Berchtold, R.P. Singh, J.S. Young, K.W. Dudeck, Polybenzimidazole composite membranes for high temperature synthesis gas separations, J. Membr. Sci. 415–416 (2012) 265–270.
[5] D.R. Pesiri, B. Jorgensen, R.C. Dye, Thermal optimization of polybenzimidazole meniscus membranes for the separation of hydrogen, methane, and carbon dioxide, J. Membr. Sci. 218 (2003) 11–18.
[6] R.P. Singh, G.J. Dahe, K.W. Dudeck, C.F. Welch, K.A. Berchtold, High temperature polybenzimidazole hollow fiber membranes for hydrogen separation and carbon dioxide capture from synthesis gas, Energy Proc. 63 (2014) 153–159.
[7] S.C. Kumbharkar, Y. Liu, K. Li, High performance polybenzimidazole based asymmetric hollow fibre membranes for H2/CO2 separation, J. Membr. Sci. 375 (2011) 231–240.
[8] C. Bas, R. Mercier, C. Dauwe, N.D. Albérola, Microstructural parameters controlling gas permeability and permselectivity in polyimide membranes, J. Membr. Sci. 349 (2010) 25–34.
[9] Y. Kase, Gas separation by polyimide membranes, in: Advanced Membrane Technology and Applications, John Wiley & Sons, Inc., 2008, pp. 581–598.
[10] X. Li, R.P. Singh, K.W. Dudeck, K.A. Berchtold, B.C. Benicewicz, Influence of polybenzimidazole main chain structure on $H_2/CO_2$ separation at elevated temperatures, J. Membr. Sci. 461 (2014) 59–68.
[11] S.C. Kumbharkar, P.B. Karadkar, U.K. Kharul, Enhancement of gas permeation properties of polybenzimidazoles by systematic structure architecture, J. Membr. Sci. 286 (2006) 161–169.
[12] H. Borjigin, K.A. Stevens, R. Liu, J.D. Moon, A.T. Shaver, S. Swinnea, B.D. Freeman, J.S. Riffle, J.E. McGrath, Synthesis and characterization of polybenzimidazoles derived from tetraaminodiphenylsulfone for high temperature gas separation membranes, Polymer 71 (2015) 135–142.
[13] J.R. Klaehn, C.J. Orme, E.S. Peterson, Blended polybenzimidazole and melamine-co-formaldehyde thermosets, J. Membr. Sci. 515 (2016) 1–6.
[14] S.S. Hosseini, T.S. Chung, Carbon membranes from blends of PBI and polyimides for $N_2/CH_4$ and $CO_2/CH_4$ separation and hydrogen purification, J. Membr. Sci. 328 (2009) 174–185.
[15] J.R. Klaehn, T.A. Luther, C.J. Orme, M.G. Jones, A.K. Wertsching, E.S. Peterson, Soluble N-Substituted organosilane polybenzimidazoles, Macromolecules 40 (2007) 7487–7492.
[16] S.C. Kumbharkar, U.K. Kharul, New N-substituted ABPBI: synthesis and evaluation of gas permeation properties, J. Membr. Sci. 360 (2010) 418–425.
[17] S.C. Kumbharkar, U.K. Kharul, Investigation of gas permeation properties of systematically modified polybenzimidazoles by N-substitution, J. Membr. Sci. 357 (2010) 134–142.
[18] S.H. Han, J.E. Lee, K.-J. Lee, H.B. Park, Y.M. Lee, Highly gas permeable and microporous polybenzimidazole membrane by thermal rearrangement, J. Membr. Sci. 357 (2010) 143–151.

[19] T. Yang, T.-S. Chung, High performance ZIF-8/PBI nano-composite membranes for high temperature hydrogen separation consisting of carbon monoxide and water vapor, Int. J. Hydrog. Energy 38 (2013) 229–239.
[20] T. Yang, G.M. Shi, T.-S. Chung, Symmetric and asymmetric zeolitic imidazolate frameworks (ZIFs)/polybenzimidazole (PBI) nanocomposite membranes for hydrogen purification at high temperatures, Adv. Energy Mater. 2 (2012) 1358–1367.
[21] L.M. Robeson, The upper bound revisited, J. Membr. Sci. 320 (2008) 390–400.
[22] L. Xiao, H. Zhang, E. Scanlon, L.S. Ramanathan, E.-W. Choe, D. Rogers, T. Apple, B.C. Benicewicz, High-temperature polybenzimidazole fuel cell membranes via a sol–gel process, Chem. Mater. 17 (2005) 5328–5333.
[23] S. Yu, H. Zhang, L. Xiao, E.W. Choe, B.C. Benicewicz, Synthesis of Poly (2,2′-(1,4-phenylene) 5,5′-bibenzimidazole) (para-PBI) and phosphoric acid doped membrane for fuel cells, Fuel Cells 9 (2009) 318–324.
[24] S.W. Chuang, S.L.C. Hsu, Synthesis and properties of a new fluorine-containing polybenzimidazole for high-temperature fuel-cell applications, J. Polym. Sci. Pol. Chem. 44 (2006) 4508–4513.
[25] G. Qian, B.C. Benicewicz, Synthesis and characterization of high molecular weight hexafluoroisopropylidene-containing polybenzimidazole for high-temperature polymer electrolyte membrane fuel cells, J. Polym. Sci. Pol. Chem. 47 (2009) 4064–4073.
[26] Y. Yuan, F. Johnson, I. Cabasso, Polybenzimidazole (PBI) molecular weight and Mark-Houwink equation, J. Appl. Polym. Sci. 112 (2009) 3436–3441.
[27] C.B. Shogbon, J.-L. Brousseau, H. Zhang, B.C. Benicewicz, Y.A. Akpalu, Determination of the molecular parameters and studies of the chain conformation of polybenzimidazole in DMAc/LiCl, Macromolecules 39 (2006) 9409–9418.
[28] H. Zhang, Novel Phosphoric Acid Doped Polybenzimidazole Membranes for Fuel Cells, Thesis, University of South Carolina, 2004.
[29] P. Musto, F.E. Karasz, W.J. MacKnight, Fourier transform infrared spectroscopy on the thermooxidative degradation of polybenzimidazole and of a polybenzimidazole/poly(ether imide) blend, Polymer 34 (1993) 2934–2945.